



## Accurate Measurement of Free Energies of Self-Assembling Systems by Computer Simulation

M. Müller, K. Ch. Daoulas

published in

*NIC Symposium 2008*,  
G. Münster, D. Wolf, M. Kremer (Editors),  
John von Neumann Institute for Computing, Jülich,  
NIC Series, Vol. 39, ISBN 978-3-9810843-5-1, pp. 255-262, 2008.

© 2008 by John von Neumann Institute for Computing  
Permission to make digital or hard copies of portions of this work for  
personal or classroom use is granted provided that the copies are not  
made or distributed for profit or commercial advantage and that copies  
bear this notice and the full citation on the first page. To copy otherwise  
requires prior specific permission by the publisher mentioned above.

<http://www.fz-juelich.de/nic-series/volume39>

# Accurate Measurement of Free Energies of Self-Assembling Systems by Computer Simulation

Marcus Müller and Kostas Ch. Daoulas

Institut für Theoretische Physik, Georg-August Universität  
Friedrich-Hund-Platz 1, D-37077 Göttingen, Germany  
*E-mail: mmueller@theorie.physik.uni-goettingen.de*

A method for calculating free energy differences between disordered and ordered phases of self-assembling systems is discussed. Applying an external, ordering field, we impose a pre-defined structure onto the fluid in the disordered phase. The structure in the presence of the external, ordering field closely mimics the structure of the ordered phase (in the absence of an ordering field). Subsequently, we gradually switch off the external, ordering field and, in turn, increase the control parameter that drives the self-assembly. The free energy difference along this reversible path connecting the disordered and the ordered state is obtained via thermodynamic integration or expanded ensemble simulation techniques in conjunction with successive umbrella sampling.

## 1 Introduction

Computer simulations provide accurate information about the statistical mechanics and thermodynamics without the need to invoke approximations that are often required to make progress in analytical calculations. The measurement of free energies, however, is a challenge because free energy differences cannot simply be expressed as functions of the particles' coordinates. Special simulation techniques have to be devised in order to extract free energy differences from particle simulations.<sup>1</sup>

In this report, we present a method that enables us to accurately calculate the free energy differences between self-assembled morphologies in amphiphilic systems. This is a computationally difficult problem for two reasons: (i) Due to the mismatch of the periodicity of the self-assembled morphology with the size of the simulation cell, there are strong finite-size effects.<sup>2</sup> Calculations with variable box shape can mitigate this problem,<sup>3,4</sup> and we do not consider this important aspect further here. (ii) Another problem stems from the absence of a well-ordered reference state – the analog of a crystal – for which the free energy can be accurately calculated. If the absolute free energy of such a reference state in the ordered phase was known, one could utilize thermodynamic integration to calculate the free energy at different state points (e.g. temperatures) and accurately map out the phase diagram without relying on the observation of hysteresis.

It is interesting to draw a comparison between self-assembly in soft matter (e.g., lamellar ordering in a diblock copolymer melt) and crystallization in simple, hard condensed matter systems (e.g., a Lennard-Jones crystal). The local difference of volume fraction,  $\phi(\mathbf{r})$ , of the two species of the amphiphilic system plays a similar role as the density of a hard crystal. Its dominant Fourier mode is the order parameter of the transition. In a well-ordered, hard crystal, each particle fluctuates little around its corresponding crystal lattice position. Thus, the system resembles an Einstein crystal, in which non-interacting particles are tethered by harmonic springs to their ideal lattice positions. Frenkel and Ladd

have used thermodynamic integration from this Einstein crystal to the well-ordered solid for calculating the absolute free energy of a hard crystal.<sup>5</sup>

In a self-assembling soft matter system, the composition also fluctuates little around the ideally ordered value, however, the molecules are in a liquid state, i.e. they diffuse and are not “tethered” to ideal positions. Therefore, there exists no well-defined reference state and previous simulation techniques for calculating the absolute free energy of hard crystals do not straightforwardly carry over to self-assembling soft matter systems.

In fact, even calculating the free energy of a homogeneous melt without repulsion between the two different monomeric species (i.e.,  $\chi N = 0$ ), which would be the analog of an ideal gas in a simple, hard condensed matter system, is a formidable task. In a liquid, the (bonded and non-bonded) interactions of a segment with its surroundings are of the order  $k_B T$ , where  $k_B$  and  $T$  are Boltzmann’s constant and temperature, respectively. Thus, the free energy per molecule is proportional to  $k_B T N$  where  $N$  denotes the number of segments (or coarse-grained interaction centres) each molecule is comprised of. In order to accurately determine the location of phase boundaries, calculate the free energy costs of defects or grain boundaries, and assess the thermodynamic stability of morphologies, one needs to know the free energy per molecule with an accuracy of  $\mathcal{O}(10^{-3} k_B T)$ . Therefore the absolute free energy would be required to be known with a precision of the order  $10^{-3}/N \approx 10^{-5}$ . The free energy difference between the disordered phase and a self-assembled structure, however, is only of the order  $\chi N k_B T \sim k_B T$ . Thus, it is advantageous to directly calculate the free energy difference between the disordered and ordered state rather than to determine it as a difference of two large absolute free energies.

Here we present a general thermodynamic integration scheme that enables us to calculate the free energy *difference* between a disordered and a spatially structured phase. We illustrate the method by studying a symmetric diblock copolymer melt. We convert the disordered melt ( $\chi_{\text{init}} N < \chi_{\text{ODT}} N$ ) into the spatially structured phase ( $\chi_{\text{final}} N > \chi_{\text{ODT}} N$ ) via a *reversible path*. Our method is inspired by the work of Sheu, Mou and Lovett calculating the absolute free energy of a Lennard-Jones solid<sup>6</sup>. Related reversible integration paths between a solid and a liquid have been used by others<sup>7,8</sup> for calculating the free energy difference between a solid and a liquid.

First, as illustrated in Fig. 1, we structure the homogeneous, disordered melt at low incompatibility,  $\chi_{\text{init}} N$ , between the two species by applying an external, ordering field,  $h(\mathbf{r})$ , conjugated to the order parameter of the transition. Ref. 6 demonstrated that the optimal choice of this ordering field,  $h$ , is such that the order parameter at  $\chi_{\text{init}} N$  in the presence of the ordering field closely mimics the order parameter at the final self-assembled state,  $\chi_{\text{final}} N$ , in the absence of the ordering field. The structure formation in response to the ordering field is completely gradual and free of any thermodynamic singularities. Second, we gradually reduce the ordering field and, in turn, increase the incompatibility between the two species. Optimally, the spatial order parameter does not vary along this path. The absence of abrupt changes in the order parameter,  $\phi(\mathbf{r})$ , or any other quantities indicates the lack of thermodynamical singularities along the second branch of the path. Thus, one turns a disordered system into a spatially ordered one without passing through a first-order transition.<sup>6</sup>

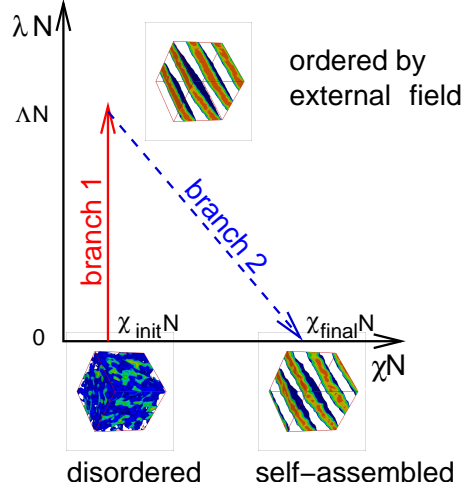


Figure 1. Sketch of the reversible path that connects the homogeneous, disordered state, the externally ordered and the self-assembled state. Configuration snapshots of a symmetric diblock melt illustrate the different states. In the snapshots three-dimensional contour plots of the composition are shown. The  $B$ -rich component is removed for clarity and the interface between the different components is coloured blue.  $\chi_{\text{init}}N = 0$ ,  $\chi_{\text{final}}N = 20$ , and the maximal strength of the ordering field is  $\Delta N = 20$ . The linear extension of the simulation cell is  $L = 7.77R_{eo}$  and the lamellar spacing is  $L_o = L/(2\sqrt{2}) = 1.686R_{eo}$ .

## 2 Model and Technique

Our thermodynamic integration scheme can be applied to different models including coarse-grained, particle-based models of amphiphilic systems and membranes<sup>9</sup> as well as field-theoretic representations<sup>10</sup>. It can be implemented in Monte Carlo or Molecular Dynamics or DPD simulations, as well as Single-Chain-in-Mean-Field (SCMF) simulations,<sup>11,12</sup> field-theoretic simulations<sup>10</sup>, and external potential dynamics<sup>13,14</sup> or dynamic density functional theory.<sup>15</sup>

In the following, we consider a liquid of  $n$  diblock copolymer molecules in a volume,  $V$ . Let the order parameter,  $\phi(\mathbf{r})$ , denote the difference of the local volume fractions of the two components, and  $\chi N$  the incompatibility of the two components per molecule. The energy of the system takes the form  $\mathcal{H} = \mathcal{H}_{\text{liq}} + \mathcal{H}_{\text{ord}} + \mathcal{H}_{\text{ext}}$ .

$$\mathcal{H}_{\text{liq}} = \mathcal{H}_{\text{b}} + \mathcal{H}_{\text{nb}} \quad \text{with} \quad \frac{\mathcal{H}_{\text{b}}}{k_B T} = \sum_{i=1}^n \sum_{s=1}^N \frac{3(N-1)}{2R_{eo}^2} [\mathbf{r}_i(s) - \mathbf{r}_i(s+1)]^2 \quad (1)$$

The bonded, intramolecular interactions,  $\mathcal{H}_{\text{b}}$ , take the form of a discretized Edwards-Hamiltonian. The shape of a flexible macromolecule is Gaussian and characterized by its mean squared end-to-end distance,  $R_{eo}$ . We discretize the contour of the symmetric diblock copolymer into  $N = 16 + 16$  coarse-grained segments. The coarse-grained parameter of relevance for matching our simulation data to experiments is the invariant degree of polymerization,  $\bar{N} = (nR_{eo}^3/N)^2 = 14\,884$ . This value lies in the typical experimental

range, and we achieve this large value not by using a particularly fine discretization,  $N$ , along the molecules but rather by increasing the polymer density,  $n/V$ .

We calculate the coarse-grained compositions from the microscopic molecular conformations,  $\{\mathbf{R}_i\}$ , using a simple cubic grid with mesh size,  $\Delta L$ , i.e., the grid contains  $N_{\text{cells}} = V/\Delta L^3$  cells.  $\Delta L = 0.19875R_{eo}$  provides sufficient spatial resolution. The local composition,  $\phi_A(\mathbf{j})$ , at a grid point,  $\mathbf{r}_j = j_x\hat{\mathbf{x}} + j_y\hat{\mathbf{y}} + j_z\hat{\mathbf{z}}$  ( $j_x, j_y, j_z$ , being multiples of  $\Delta L$ , index the grid point and  $\hat{\mathbf{x}}, \hat{\mathbf{y}}, \hat{\mathbf{z}}$  denotes the unit cell vectors of the simple cubic lattice, respectively) is given by  $\phi_A(\mathbf{j}) = \frac{V}{nN\Delta L^3} \sum_{i=1}^n \sum_{s=1}^{fN} m(\mathbf{r}_i(s) - \mathbf{r}_j)$ , and a similar expression holds for the local volume fraction of the  $B$  component. The assignment function,  $m$ , characterizes the mapping of the continuous, off-lattice segment coordinates onto the coarse-grained grid and we utilize a linear particle-mesh extrapolation.<sup>16</sup>

The small compressibility of a dense polymer liquid is captured by the non-bonded interactions of Helfand-type:  $\frac{\mathcal{H}_{\text{nb}}}{nk_B T} = \frac{\kappa_o N}{2} \frac{1}{N_{\text{cells}}} \sum_{\mathbf{j}} [\phi_A(\mathbf{j}) + \phi_B(\mathbf{j}) - 1]^2$ . The value  $\kappa_o N = 50$  is sufficient to suppress fluctuations of the total density on the length scale of a small fraction of  $R_{eo}$ .

The incompatibility between unlike segments,  $A$  and  $B$ , is described by the most symmetric choice:  $\frac{\mathcal{H}_{\text{ord}}}{nk_B T} = -\frac{\chi N}{N_{\text{cells}}} \sum_{\mathbf{j}} \phi^2(\mathbf{j})$  with  $\phi(\mathbf{j}) = \frac{\phi_A(\mathbf{j}) - \phi_B(\mathbf{j})}{2}$ . In addition, we apply an external, ordering field,  $h(\mathbf{r}) = -\lambda N f_{\text{ext}}(\mathbf{r})$ , that linearly couples to the order parameter. It results in an energy contribution of the form  $\frac{\mathcal{H}_{\text{ext}}}{nk_B T} = -\frac{\lambda N}{V} \int_V d^3\mathbf{r} f_{\text{ext}}(\mathbf{r})\phi(\mathbf{r})$  where  $\lambda N$  characterizes the strength and  $f_{\text{ext}}$  the spatial variation of the ordering field.

These interactions define a coarse-grained model that can be very efficiently studied by computer simulations because (i) the interactions are soft, (ii) the absence of harsh excluded volume interactions allows for a high polymer density and an invariant degree of polymerization that is comparable to experimental values, and (iii) the calculation of the non-bonded interactions via a coarse-grained grid speeds up the calculation of the energy by about two orders of magnitudes in dense systems.<sup>12</sup> The model is simulated by Single-Chain-in-Mean (SCMF) simulations<sup>12,11</sup> where the explicit chain conformations evolve in time via a Smart Monte Carlo algorithm.<sup>17</sup>

For this model, the free energy changes along the two branches depicted in Fig. 1 take the simple, explicit form

$$\frac{\Delta F_1}{nk_B T} = - \int_0^{\Lambda N} d\lambda N \left\langle \frac{1}{N_{\text{cells}}} \sum_{\mathbf{j}} f_{\text{ext}}(\mathbf{j})\phi(\mathbf{j}) \right\rangle \Big|_{\chi_{\text{init}} N} \quad (2)$$

$$\frac{\Delta F_2}{nk_B T} = - \int_{\Lambda N}^0 d\lambda N \left\langle \frac{1}{N_{\text{cell}}} \sum_{\mathbf{j}} (f_{\text{ext}}(\mathbf{j})\phi(\mathbf{j}) - \phi^2(\mathbf{j})) \right\rangle \quad (3)$$

We simulate the systems for different state points along the integration path, measure the integrands of Eqs. (2) and (3), and evaluate the free energy changes by numerically evaluating the integrals. This provides a first estimate for the free energy changes along the path. Subsequently, we employ an expanded ensemble<sup>18</sup> where the incompatibility,  $\chi N$ , and the strength of the external field,  $\lambda N$ , vary along the integration path. Within a single simulation run the system will visit different state points along the integration path. To this end, the Monte Carlo algorithm comprises additional moves that alter  $\chi N$  and  $\lambda N$ . The expanded partition function takes the form

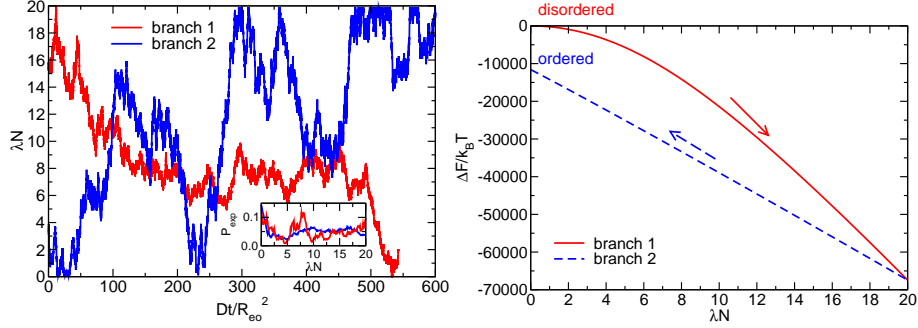


Figure 2. a) Evolution of the ordering field,  $\lambda N$ , in the course of the expanded ensemble simulation along both branches. The “time” is measured in units of the Rouse-time of the macromolecules. The inset presents the probability distribution,  $P_{\text{exp}}(\chi N, \lambda N)$ . b) Changes of the free energy along the two branches of the integration path.

$$Z_{\text{exp}} = \sum_{(\chi N, \lambda N)} \exp \left[ \frac{w(\chi N, \lambda N)}{k_B T} \right] \int \mathcal{D}\{\{\mathbf{R}_i\}\} \exp \left[ -\frac{\mathcal{H}_{\text{liq}} + \mathcal{H}_{\text{ord}}(\chi N) + \mathcal{H}_{\text{ext}}(\lambda N)}{k_B T} \right] \quad (4)$$

The pre-weighting factors,  $w(\chi N, \lambda N)$ , facilitate transition between different states,  $(\chi N, \lambda N)$ , along the integration path. The probability,  $P_{\text{exp}}$ , of finding the system in a state characterized by  $\chi N$  and  $\lambda N$  is related to the free energy via  $P_{\text{exp}}(\chi N, \lambda N) = \frac{1}{Z} \exp \left[ -\frac{F(\chi N, \lambda N) - w(\chi N, \lambda N)}{k_B T} \right]$ . The choice,  $w(\chi N, \lambda N) \approx F(n, V, T, \chi N, \lambda N)$ , for the pre-weighting factors ensures that the different state points are sampled with approximately equal probability. Initial estimates of the pre-weighting factors are obtained by thermodynamic integration and successive umbrella sampling<sup>19</sup> but alternative schemes<sup>20,21</sup> can be envisioned. Note that compared to other re-weighting techniques (utilized e.g., to calculate phase diagrams, interface tensions, or potentials of mean force)<sup>1</sup> the free energy difference along the integration path is large,  $\mathcal{O}(10^4 k_B T)$ , and a systematic method for obtaining/improving the pre-weighting factors is required.

### 3 Results

In order to calculate the free energy difference between the disordered state,  $\chi N = 0$ , and the lamellar ordered structure at  $\chi N = 20$ , we discretize both branches of the integration path. The variation of the integrands along both branches of the path is completely gradual, indicating the absence of a first-order transition. The absence of a first-order transition is corroborated by Fig. 2a, where we show the evolution of the strength of the ordering field,  $\lambda N$ , during the course of the expanded ensemble simulation. The simulation data presented correspond to a single configuration that samples all different external field strengths,  $\lambda N$ , of a branch.

The system freely diffuses along the  $\lambda N$ -axis and there is no “kinetic barrier” between neighbouring  $\lambda N$ -states. This observation demonstrates that the regions of configuration

space associated with neighbouring  $\lambda N$ -values overlap. We also observe that the system visits all  $\lambda N$ -states with roughly equal probability (see inset). This demonstrates that the pre-weighting factors are very accurate and the error in the free energy difference is of the order of a few  $k_B T$  which, in turn, is much smaller than the total free energy difference,  $\mathcal{O}(10^4)k_B T$ .

The SCMF simulations can be very efficiently implemented on a parallel computer because we simulate an ensemble of independent molecules in fluctuating fields.<sup>11,12</sup> Even for the rather small system size considered in this work, 32 processors can be used. If one takes the absence of a free energy barrier along the thermodynamic integration path for granted, it would be beneficial to subdivide the range of external field strength and use a successive umbrella sampling technique.<sup>19</sup> In this case, the  $\sim 400$  points along the two branches can be divided into several sub-branches (typically, we use 32) that overlap at their boundaries. Each sub-branch can be assigned to a different group of processors. Additionally, we have implemented a parallel-tempering scheme to facilitate the relaxation of the systems by exchanging configurations between different sub-branches. This allows us to efficiently employ  $32^2 = 1024$  processors.

In Fig. 2b, the variation of the free energy along the two branches is presented. Since we calculate free energy differences, we arbitrarily set the free energy of the initial, disordered state ( $\chi N = 0$ ) to zero, and we have matched the free energy at the end of the first branch with that of the beginning of the second one. From the data we obtain a free energy difference of  $\Delta F/k_B T = 11607(10)$  or  $\Delta F/nk_B T = -0.87659(75)$  for a lamellar spacing,  $L_o = 1.686R_{eo}$ . The error estimate refers to the statistical error of the result but does not include a possible systematic over-estimation of the free energy because of the deviation of the lamellar spacing from its equilibrium value due to the finite size of the simulation cell.

## 4 Outlook

This new simulation technique permits us to accurately calculate free energy differences in self-assembling soft matter. Potential application encompass the determination of phase diagrams and the identification of stable phases. Applying the scheme to a perfectly ordered system and a system with an interface (e.g., between self-assembled phases with different orientations), one can calculate the free energy of grain boundaries and defects. The calculation of the free energy of a grain boundary is illustrated in Fig. 3. Calculating the free energy difference between a disordered system,  $\chi N = 0$ , and an ordered system,  $\chi N = 20$  with and without grain boundary we obtain the free energy difference  $\Delta F = 0.032k_B T/\text{chain}$ . This value corresponds to an interface free energy,  $\frac{\gamma R_{eo}^2}{k_B T \sqrt{N}} = 0.16$ . This value is slightly smaller than the value 0.21 predicted by SCF theory.<sup>22</sup> This deviation is due to (i) fluctuations that tend to reduce the free energy and (ii) the differences in the models used in SCF theory and SCMF simulations. While SCF theory assumes zero-ranged interactions, the spatial range of interactions in the SCMF simulations is set by the rather coarse grid spacing,  $\Delta L$ .

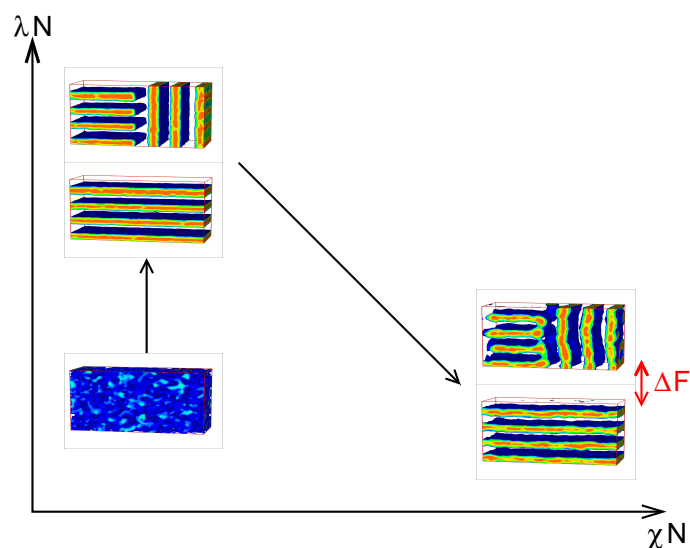


Figure 3. Illustration of the thermodynamic integration path for calculating the free energy difference of a T-junction between two lamellar domains of perpendicular orientation at  $\chi N = 20$  and  $N = 14884$ . The simulation cell of geometry  $4 \times 10.2 \times 6.8R_{eo}^3$  contains 33 848 polymers with  $N = 32$  segments.

## Acknowledgments

It is a great pleasure to thank M.P. Allen, K. Binder, G.H. Fredrickson, and M.W. Matsen for fruitful discussions. Financial support was provided by the DFG priority program "Nano- and Microfluidics" under grant Mu 1674/3-2 and the Volkswagen foundation. Computing time at the John von Neumann Institute for Computing (NIC) is gratefully acknowledged.

## References

1. M. Müller and J. J. de Pablo, *Simulation techniques for calculating free energies*, *Lect. Notes Phys.*, **703**, 67–122, 2006.
2. U. Micka and K. Binder, *Unusual Finite-Size Effects in the Monte-Carlo Simulation of Microphase Formation of Block-Copolymer Melts*, *Macromolecular Theory and Simulations*, **4**, 419–447, 1995.
3. M. Murat, G. S. Grest, and K. Kremer, *Statics and Dynamics of Symmetric Diblock Copolymers: a Molecular Dynamics Study*, *Macromolecules*, **32**, 595–609, 1999.
4. C. A. Tyler and D. C. Morse, *Stress in Self-Consistent-Field Theory*, *Macromolecules*, **36**, 8184–8188, 2003.
5. D. Frenkel and A. J. C. Ladd, *New Monte Carlo Method to Compute the Free Energy of Arbitrary Solids. Application to the FCC and HCP Phases of Hard Spheres*, *J. Chem. Phys.*, **81**, 3188–3193, 1984.
6. S. Y. Sheu, C. Y. Mou, and R. Lovett, *How a solid can be turned into a gas without*



- passing through a first-order phase-transformation, *Phys. Rev. E*, **51**, R3795–R3798, 1995.
7. G. Grochola, *Constrained fluid  $\lambda$ -integration: constructing a reversible thermodynamic path between the solid and liquid state*, *J. Chem. Phys.*, **120**, 2122–2126, 2004.
  8. D. M. Eike, J. F. Brennecke, and E. J. Maginn, *Toward a Robust and General Molecular Simulation Method for Computing Solid-Liquid Coexistence*, *J. Chem. Phys.*, **122**, 014115, 2005.
  9. M. Müller, K. Katsov, and M. Schick, *Biological and Synthetic Membranes: What Can Be Learned From a Coarse-Grained Description?*, *Physics Reports*, **434**, 113–176, 2006.
  10. G. H. Fredrickson, V. Ganesan, and F. Drolet, *Field-Theoretic Computer Simulation Methods for Polymers and Complex Fluids*, *Macromolecules*, **35**, 16–39, 2002.
  11. M. Müller and G. D. Smith, *Phase Separation in Binary Mixtures containing Polymers: a Quantitative Comparison of Single-Chain-in-Mean-Field Simulations and Computer Simulations of the Corresponding Multichain Systems*, *J. Polym. Sci. B: Polymer Physics*, **43**, 934–958, 2005.
  12. K. Ch. Daoulas and M. Müller, *Single Chain in Mean Field Simulations: Quasi-Instantaneous Field Approximation and Quantitative Comparison With Monte Carlo Simulations*, *J. Chem. Phys.*, **125**, 184904, 2006.
  13. N. M. Maurits and J. G. E. M. Fraaije, *Mesoscopic Dynamics of Copolymer Melts: From Density Dynamics To External Potential Dynamics Using Nonlocal Kinetic Coupling*, *J. Chem. Phys.*, **107**, 5879–5889, 1997.
  14. E. Reister, M. Müller, and K. Binder, *Spinodal Decomposition in a Binary Polymer Mixture: Dynamic Self-Consistent-Field Theory and Monte Carlo Simulations*, *Phys. Rev. E*, **64**, 041804, 2001.
  15. J. G. E. M. Fraaije, *Dynamic Density-Functional Theory for Microphase Separation Kinetics of Block-Copolymer Melts*, *J. Chem. Phys.*, **99**, 9202–9212, 1993.
  16. J. W. Eastwood, R. W. Hockney, and D. N. Lawrence, *P3m3dp - The 3-Dimensional Periodic Particle-Particle-Particle-Mesh Program*, *Computer Physics Communications*, **19**, 215–261, 1980.
  17. P. J. Rossky, J. D. Doll, and H. L. Friedman, *Brownian Dynamics As Smart Monte-Carlo Simulation*, *J. Chem. Phys.*, **69**, 4628–4633, 1978.
  18. A. P. Lyubartsev, A. A. Martsinovski, S. V. Shevkunov, and P. N. Vorontsov-Velyaminov, *New approach to Monte-Carlo calculation of the free-energy – Method of expanded ensembles*, *J. Chem. Phys.*, **96**, 1776–1783, 1992.
  19. P. Virnau and M. Müller, *Calculation of Free Energy Through Successive Umbrella Sampling*, *J. Chem. Phys.*, **120**, 10925–10930, 2004.
  20. B. A. Berg, *Multicanonical recursions*, *J. Stat. Phys.*, **82**, 323, 1996.
  21. F. G. Wang and D. P. Landau, *Efficient Multiple-Range Random Walk Algorithm to Calculate the Density of States*, *Phys. Rev. Lett.*, **86**, 2050–2053, 2001.
  22. D. Duque, K. Katsov, and M. Schick, *Theory Of T Junctions And Symmetric Tilt Grain Boundaries In Pure And Mixed Polymer Systems*, *J. Chem. Phys.*, **117**, 10315–10320, 2002.